Am J Cancer Res 2021;11(10):4981-4993
www.ajcr.us /ISSN:2156-6976/ajcr0135488

Original Article

HuR enhances FSTL1 transcript stability to promote invasion and metastasis of squamous cell carcinoma

Gopinath M Sundaram[1*], Shan Quah[1*], Lum Guo Guang[1], Prabha Sampath[1,2,3]

*[1]Skin Research Institute of Singapore, Agency for Science Technology & Research (A*STAR), Singapore 138648, Singapore; [2]Department of Biochemistry, Yong Loo Lin School of Medicine, National University of Singapore, Singapore 117596, Singapore; [3]Program in Cancer and Stem Cell Biology, Duke-NUS Medical School, 8 College Road, Singapore 169857, Singapore. [*]Equal contributors.*

Received May 20, 2021; Accepted July 16, 2021; Epub October 15, 2021; Published October 30, 2021

Abstract: Squamous cell carcinoma (SCC) is a lethal malignancy with a high propensity for metastasis. Follistatin-like 1 (FSTL1), a pro-metastatic glycoprotein, is absent from healthy epithelia and aberrantly upregulated in SCC. The *FSTL1* transcript encodes two alternative gene products whose dominance is post-transcriptionally regulated via a bistable switch. In healthy epithelia, *FSTL1 mRNA* is destabilized by binding of KH-type splicing regulatory protein (KSRP), and processed as a primary microRNA encoding miR-198. In SCC, KSRP downregulation terminates miR-198 processing, enabling FSTL1 translation. Here, we identify HuR (Human Antigen R) as an upstream regulator of FSTL1 and describe how downregulation of KSRP is permissive, but not sufficient, to promote sustained FSTL1 expression. Moreover, we demonstrate how the interplay between two RNA-binding proteins controls the translation of pro-oncogenic FSTL1. Increased expression of HuR in SCC outcompetes KSRP and enhances *FSTL1* transcript stability, enabling persistent FSTL1 expression and activation of downstream metastatic pathways.

Keywords: MicroRNA, squamous cell carcinoma, cell proliferation, metastasis, cancer, RNA-binding proteins

Introduction

Squamous cell carcinomas (SCCs) manipulate several aspects of the wound healing program to promote metastasis. We have previously shown that a dual-state molecular switch activates keratinocyte migration during wound closure [1], and that the same switch is hijacked by SCC cells to drive metastasis [2]. A single transcript - *FSTL1* - lies at the heart of this switch. *FSTL1* belongs to a unique class of messenger RNAs (mRNAs) which can also encode exonic microRNA (miRNA). The transcript can generate two alternate gene products. It may either be processed to produce the miR-198 miRNA or translated to express FSTL1 protein. Follistatin-like 1 (FSTL1), a secreted glycoprotein with pro-migratory roles in SCC, is aberrantly expressed in many cancers including SCC [3-7]. In contrast, miR-198 suppresses keratinocyte migration [1].

FSTL1 and miR-198 show context-specific alternative expression that is instrumental to timely repair of epithelial damage. The dominant product in healthy epithelia is miR-198. Upon wounding, miR-198 processing is downregulated in favour of FSTL1 translation. This enhances temporal cell migration and wound re-epithelialization [1]. This mechanism is hijacked in SCC. EGF signalling and blocks miR-198 expression and enables sustained FSTL1 translation [2]. Aberrantly overexpressed FSTL1 coordinates a suite of pro-metastatic processes ranging from immune evasion to direct stimulation of tumour cell migration and invasion [2, 8]. Mitigating FSTL1 expression in SCC would reduce the activation of such pathways and has been proposed to be of clinical benefit as anticancer therapy [8]. However, before pursuing FSTL1 as an anticancer target, we will need a detailed picture of the molecular pathways underlying its dysregulation in SCC.

At the core of the FSTL1 regulatory network is the *FSTL1* transcript itself. *FSTL1* transcript stability is modulated by RNA-binding proteins. In healthy epithelia, the *FSTL1* transcript is

destabilized by the binding of KH-type splicing regulatory protein (KSRP), which activates miR-198 processing [1]. In SCC, epidermal growth factor (EGF) signalling stops miR-198 production by downregulating KSRP [2]. It is currently unclear whether blocking miR-198 processing alone is sufficient to enable FSTL1 mRNA stabilization, export, and translation, or whether additional molecular regulation is required for these processes to occur. Here, we present evidence that HuR acts as an upstream regulator of the molecular switch and binds to *FSTL1 mRNA* through a uridylate-rich element (URE) motif. We investigate the effect of increasing HuR abundance relative to KSRP and demonstrate how high levels of HuR displace KSRP from binding to *FSTL1*. Competitive binding of HuR displaces KSRP, prevents expression of miR-198, stabilizes the *FSTL1* transcript, and enables sustained FSTL1 protein expression.

Materials and methods

Cell culture and SCC tissue arrays

SCC cell lines (A253, SCC12, SCC13) were cultured in RM^+ media (3:1 DMEM; F12 HAMS media supplemented with 10% FBS, 0.5 µg/ml hydrocortisone, 5 µg/ml of insulin and transferrin, 13 ng/ml liothyronin, 1% glutamine, 10 ng/ml epidermal growth factor and penicillin/streptomycin). A tissue array (SK802a) containing cutaneous squamous cell carcinoma sections (76 cutaneous SCC tissue sections, 2 normal sections adjacent to tumour and 2 normal skin sections) was obtained from US Biomax. Three cSCC sections were negative for KRT14 and therefore omitted for further study. Human foreskin dermal fibroblasts and lenti-X 293T (Clontech) were cultured in DMEM supplemented with 10% FCS and penicillin/streptomycin.

Antibodies

Antibodies used in this study are as follows. Goat anti-FSTL1 antibody (#ab11805, Abcam), Rabbit anti-DIAPH1 antibody (#5486, Cell Signalling), Mouse anti-LAMC2 antibody (#sc25-341, Santacruz biotechnologies), Rabbit anti-PLAU (#ab24121, Abcam), Rabbit anti-KSRP antibody (#A302-22A, Bethyl laboratories), Rabbit anti-HuR antibody (#ab85539), mouse anti-KRT14 (clone LLO01). Chicken anti-goat Alexa Fluor 488, Donkey anti-rabbit and anti-mouse Alexa Fluor 488 and Alexa Fluor 555 secondary antibodies (Molecular Probes) were used as secondary antibodies in immunohistochemistry.

Boyden chamber invasion assays

In vitro invasion assays were performed in BD BioCoat Matrigel invasion assay chambers. Two days post transduction, cells were harvested and seeded onto the upper chamber in RM^+ media without serum. Complete RM^+ medium was used as a chemo-attractant in the lower chambers. 20 h post-seeding, cells on the upper membrane surface were removed with a cotton swab and the invaded cells were fixed in methanol and stained with Giemsa solution. Cell invasion was expressed as the percentage of cells invaded in six microscopic fields per chamber in three biological replicates. Invaded cell numbers in control cells were considered as 100%.

Organotypic invasion assay and quantification

Organotypic assays were set up as described by Gaggioli et al, (2007) with minor modifications. Briefly, in ice cold conditions, equal amount of matrigel (#354234 BD Biosciences) and Rat tail collagen type I (#354236 BD Biosciences) with one tenth volume of FCS and 10 × DMEM were mixed and pH adjusted to neutral by addition of 0.1 N NaOH. About 800 µl of this solution was added to millicell hanging cell culture inserts and placed in 12 well plates (Nunc) for 1 hr at 37°C for solidification. Complete fibroblast medium was added to both top and bottom of the insert and left overnight at 37°C. Human dermal fibroblasts (1×10^5) was mixed with SCC12 or SCC13 cell line (2.5×10^5) and seeded onto the gel and allowed to grow submerged in RM^+ medium for 24 hrs. Inserts were lifted to air liquid interface the very next day and cultures were maintained in RM^- media (RM^+ media without epidermal growth factor) for two weeks after which the organotypic gels were processed for histology. FFPE Sections were stained using anti-KRT14 antibodies by immunohistochemistry to locate SCC cells. The depth of invasion and total number of Keratin-14 positive cells were quantified using Image J software.

Immunohistochemistry

Five micron tissue sections were mounted on poly L-lysine-coated glass slides (Thermo Scientific). Sections were de-paraffinized in

xylene 3 times followed by 3 washes in absolute ethanol and rehydrated using descending ethanol concentrations and finally in phosphate buffered saline (PBS). Endogenous peroxidase was quenched by immersing the slides in 3% hydrogen peroxide and methanol for 30 minutes. Antigen retrieval (dependant on the antibody), was performed using programmable pressure cooker with "target retrieval solution", pH 6.0 (Dako). Non-specific reactivity in the tissues was blocked by incubation in 10% goat serum in PBS before incubating with the primary antibody at room temperature for 2 hr. Unbound primary antibodies were removed by washing in running tap water for 10 min before incubation with species matched secondary HRP-labelled polymer antibodies (Dako). Chromogen 3,3'-diaminobenzidine (Dako) was used as substrate for colour development. Slides were counterstained with hematoxylin before dehydration and mounted with DPX (Sigma). For fluorescent immunodetection, species specific secondary antibodies conjugated to Alexa 488/555 were used instead of HRP-labeled polymer antibodies. Sections were washed with running tap water, counterstained with DAPI (100 ng/ml) and mounted using Florsave (Calbiochem) mounting medium. For experiments where goat primary antibodies were used, 5% BSA in PBS was substituted for 10% goat serum. Images were acquired on a Zeiss Axioimager microscope (for bright field imaging) or on Olympus FluoView FV1000 (for fluorescent antibody detection). Quantification of staining intensities in tissue arrays was performed visually by two independent observers. Intensities were classified as negative, week, moderate and strong by averaging the independent observations.

miRNA in situ hybridization

5 μ sections were deparaffinized and rehydrated as above and boiled in pre-treatment solution for 5 min (Panomics), washed in PBS, followed by protease (Panomics) treatment at 37°C for 30 min. Sections were incubated with LNA probes [5'-DIG labelled LNA probes specific for miR-198 or scrambled probe with no homology to known vertebrate miRNAs (Exiqon)] in hybridization buffer containing 50% Formamide (Sigma), 5 × SSC (Firstbase), 5 × Denhardts solution (Sigma), 0.25 mg/ml of denatured solman sperm DNA (Invitrogen), 0.25 mg/ml Yeast tRNA (Invitrogen), 20 μl per ml of Poly A solution (Roche DIG tailing kit) and 1% blocking solution (Roche) at 51°C for 4 hours. Following stringent wash with series of buffers containing 5 × SSC, 1 × SSC, 0.3 × SSC, sections were blocked with 10% Goat serum and further incubated with anti-DIG alkaline phosphatase (Roche) overnight at 4°C. Sections were washed in PBS-T (0.1%) and miRNA bound LNA probes were detected by Fast red substrate (Panomics). After counterstaining with DAPI, slides were mounted using FluorSave (Merck). Image acquisition was performed with Olympus FluoView FV1000 using TRITC filter.

Gel retardation assay

The pre-miR-198 substrate for gel retardation assays was prepared as described earlier [1]. The U-rich element present within pre-miR-198 sequence was replaced with a string of five C residues using the QuikChange Site-Directed Mutagenesis Kit (Agilent). Pre-miR-7 was amplified from genomic DNA using primers with a flanking T7 promoter sequence (sequences are listed in Table S1). Increasing concentration of recombinant HuR protein (0.5, 2 and 5 μM) was incubated with the wild-type or mutant pre-miR-198 transcripts in 20 μl of reaction buffer containing 30 mM Tris-HCl (pH 7.4), 5 mM $MgCl_2$, 50 mM KCl, 0.5 mM DTT, 40 U/ml of RNaseOUT, 250 μg/ml of yeast tRNA and 10% glycerol. After 30 min at room temperature, reaction products were resolved through 6% native polyacrylamide gel electrophoresis. For the competitive binding assay, 0.5 μM of KSRP was co-incubated with the indicated concentrations of HuR in the presence of pre-miR-198 transcript. Gels were dried and the protein-RNA complex and unbound RNA were visualized by phosphor imaging.

In vitro transcription and translation

Generation of pMIRGLO dual luciferase containing FSTL1 3'-untranslated region (UTR) downstream of firefly luciferase open reading frame has been described earlier [1]. Primers with T7 RNA polymerase promoter linkers (Table S1) were used to amplify the entire luciferase-FSTL1 3'-UTR fragment along with the Kozak sequence. A PCR fragment containing copGFP ORF was amplified from pCDH vector (System Biosciences) using primers listed in

Table S1. PCR products were purified and subjected to *in vitro* transcription with Ambion mMessage mMachine kit. Mutation of U-rich sequences to C residues was carried out using the QuickChange II site directed mutagenesis kit (Agilent Technologies) as per manufacturers protocol. For in vitro translation, 500 ng of purified Luc-FSTL1 chimeric RNA or URE mutant RNA and 200 ng of GFP RNA was added to 30 µl of rabbit reticulocyte lysate, 20 µM of methionine free amino acid mixture, 50 µCi of Easy tag Express ^{35}S protein labelling mix and 10 µg of cell extract in a total volume of 50 µl for 1 h at 30°C. 10 µl aliquot of the reaction mix was separated on 10% SDS-PAGE, fixed in 10% acetic acid/40% methanol, dried and subjected to autoradiography.

Luciferase reporter assays

pMIRGLO Luciferase reporter containing wild type *FSTL1* 3'UTR or URE mutant were co-transfected along with 30 nM of non-targeting siRNA or siRNA specific for HuR in 293T cells using lipofectamine 2000 (Invitrogen) as per manufacturer's protocol. Firefly and Renilla luciferase activities were measured 24 h post transfection using Dual Luciferase reporter assay system (Promega). The firefly luminescence was normalized to Renilla luminescence values as an internal control for transfection efficiency.

RNA immunoprecipitation (RIP)

SCC12 or SCC13 or A253 cells were lysed in RIPA buffer (Pierce), by mild sonication and clarified by centrifugation at 13,000 × g for 10 min. Total cell extracts were incubated with 4 µg rabbit anti-KSRP antibody (Abcam) or 4 µg of mouse anti-HuR antibody or control rabbit IgG for 3 h at 4°C. The antigen-antibody complex was retrieved using 40 µl (resin volume) of protein A Sepharose pre-blocked with yeast tRNA (50 µg/ml) and BSA (100 µg/ml) equilibrated with RIPA buffer at 4°C for 1 hr. After washing the beads with 1 ml of RIPA buffer for 3 times, immunoprecipitated RNA bound to the resin was solubilized with the lysis buffer provided in Exiqon miRcury RNA isolation kit. Total RNA was extracted. Reverse transcription of the immunoprecipitated RNA (10 µl) as well as the input extract RNA (10%) was carried out with Superscript III reverse transcriptase kit (Invitrogen). 4 µl of the cDNA was used in qRT-PCR using primers spanning Pre-miR-198 in primary transcript. Results were normalized to input RNA levels and plotted as fold enrichment compared to IgG control RIP.

Results

Aberrant expression of pro-metastatic FSTL1 correlates with increased expression of human antigen R (HuR) in SCC

The FSTL1/miR-198 wound healing switch is hijacked in head and neck SCC (HNSCC) to enhance metastasis [2]. We observed a similar scenario in cutaneous SCC (cSCC)-miR-198 was abundant in healthy epithelia but virtually absent in cSCC, with an inverse correlation to FSTL1 expression (**Figure 1A**, **1B**). In SCC, EGF downregulates KH-type splicing regulatory protein (KSRP), which is essential for processing miR-198 [1]. Although KSRP downregulation is permissive for *FSTL1* translation, it is unclear whether this is sufficient to enable sustained expression of pro-metastatic FSTL1 in SCC. To determine the underlying mechanism which facilitates transcript stabilization enabling sustained translation, we analysed *FSTL1* transcript for the presence of U-rich elements, a subclass of adenylate/uridylate-rich elements (AREs/UREs). These sequences are common in labile RNAs, where they mediate transcript stability by binding to various RNA-binding proteins (RBPs) [9]. We identified a URE (5'-UUUUU-3') within the stem-loop structure of the 3'UTR that corresponds to pre-miR-198. This site is in very close proximity to the KSRP binding site, strongly suggesting that a URE-binding protein might interact competitively with KSRP to bind to *FSTL1* (**Figure 1C**).

ELAV/Hu (embryonic lethal abnormal vision-like 1/Human antigen) is a family of RNA-binding proteins with well-documented affinity for AREs and UREs [9-11]. The most ubiquitously-expressed of these proteins is Human Antigen R (HuR), known for its role in mRNA stabilization. HuR contains three highly conserved RNA recognition motifs (RRMs), one of which (RRM3) binds to pentamer U-rich sequences [9, 12]. HuR is highly expressed in many cancers [13-17], including squamous cell carcinomas [18-20], where a number of HuR-stabilized transcripts have been found to promote the acquisition of oncogenic traits [21-23]. We hypothesize that HuR could stabilize the *FSTL1* tran-

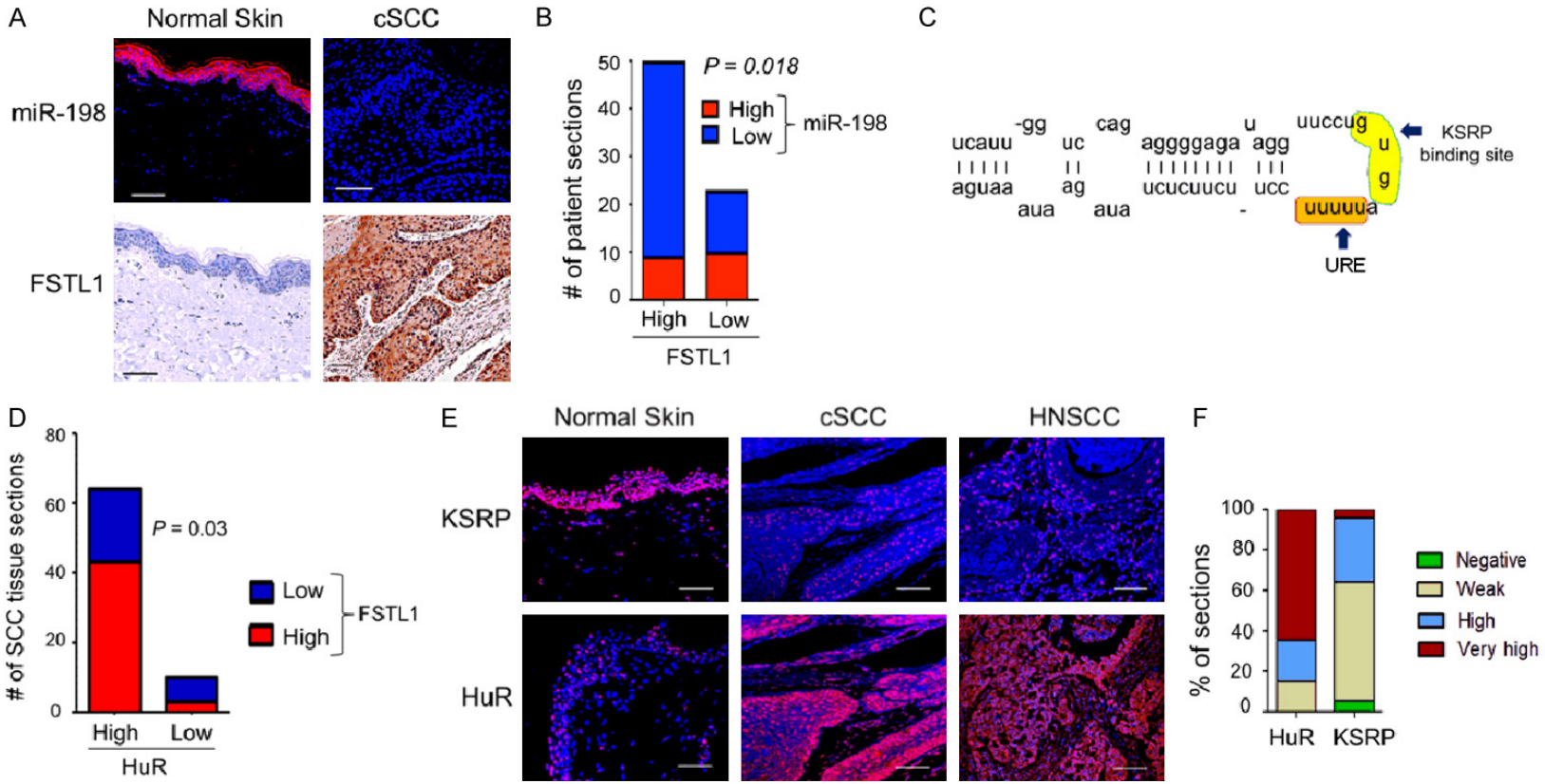

Figure 1. Aberrant expression of pro-metastatic FSTL1 correlates with increased expression of Human Antigen R (HuR) in SCC. A. *In situ* hybridization for miR-198 (upper panel) and immunohistochemical staining (lower panel) for FSTL1 in normal skin (n=5) and cSCC (n=73) tissue sections. Scale bar =100 μm. B. Bar graph showing the correlation between miR-198 and FSTL1 expression in cSCC tissue sections. P<0.05 (Chi-squared test). C. Schematic representation of the positions of KSRP and HuR binding motifs within the pre-miR-198 stem loop in the *FSTL1* 3' UTR. D. Bar graph showing the correlation between FSTL1 and HuR expression in SCC tissue sections. P<0.05 (Chi-squared test). E. Immunohistochemical staining for KSRP (upper panel) and HuR (lower panel) in normal skin (n=5) and SCC (n=86) tissue sections. Scale bar =100 μm. F. Bar graph showing the correlation between KSRP and HuR expression in SCC tissue sections. P<0.05 (Chi-squared test).

script by binding to the URE in its 3'UTR. The close proximity of the URE to the KSRP binding site further suggests that competitive binding could occur between the two proteins, which have opposing functions. If this were the case, the relative abundance of KSRP and HuR would be critical in deciding the fate of the transcript, and the consequent downstream effects on cell migratory behaviour.

In line with our hypothesis, we observed a clear positive correlation in the expression of HuR and FSTL1 in SCC sections (**Figure 1D**). We observed an obvious inverse correlation in the expression of HuR versus KSRP (**Figure 1E**, **1F**), and confirmed enhanced expression of HuR in SCC (**Figure 1E**, lower panel). Taken together, these observations suggest that upregulation of HuR and downregulation of KSRP in SCC would favour HuR binding, *FSTL1* translation, and its consequent downstream effects on metastasis.

HuR is pro-invasive and knockdown of HuR phenocopies FSTL1 knockdown

To confirm that HuR enhances metastasis [19, 21] we studied the effects of HuR knockdown on invasion in SCC cells. Short hairpin RNAs (shRNAs) targeting either FSTL1 or HuR were stably expressed in SCC cell lines (Figure S1A). In a 2-dimensional scratch wound assay, we observed that cell migration was significantly impeded in the presence of shHuR, relative to the same cells expressing a control shRNA (**Figure 2A**). Using Boyden chamber invasion assays, we showed that knockdown of either FSTL1 or HuR significantly reduced the total number of successfully invading cells relative to the control shRNA (**Figure 2B**, **2C**). A three-dimensional organotypic assay mimicking *in vivo* stromal invasion [24], further confirmed that HuR is pro-invasive, and that knockdown of HuR phenocopies FSTL1 knockdown (**Figures 2D**, S1B). These observations suggest that HuR is an upstream regulator of FSTL1 and HuR may exert its pro-metastatic effects through FSTL1. Analysis of 'The Cancer Genome Atlas' (TCGA) database clearly indicates increased expression of HuR in SCC patient samples compared to normal tissue (**Figure 2E**). A significant increase in *HuR* transcript abundance with nodal metastasis in HNSCC support a pro-invasive role for HuR (**Figure 2F**); all emphasize the clinical significance of HuR-mediated modulation of the molecular switch leading to enhanced metastasis.

Thus, it is evident that HuR promotes the migration and invasion of SCC cells without affecting their proliferation (Figure S2). This is akin to the function of FSTL1 which promotes cell migration and invasion without an overt effect on proliferation [1, 2]. Due to the pleiotropic effects of HuR, these properties might be conferred through one or more parallel pathways, such as those already described in the literature [21]. The similar effects of HuR and FSTL1 knockdown suggest that HuR may exert its pro-metastatic effects through FSTL1. In order to test this hypothesis, we looked at the interaction between HuR and the *FSTL1* transcript.

The interplay between two RNA-binding proteins controls the fate of FSTL1 transcript

We examined the interaction between HuR and *FSTL1* by performing RNA immunoprecipitation (RIP) followed by quantitative RT-PCR (qRT-PCR) on cell lysates from SCC12 cells (**Figure 3A**). A significant enrichment of the *FSTL1* transcript with an anti-HuR antibody, but not with the control IgG, confirmed that HuR binds to *FSTL1* mRNA and directly interacts with FSTL1. Enrichment of *KRT6A* was not observed, confirming the specificity of this interaction (**Figure 3A**). Identical results were also obtained in SCC13 and A253 cells (Figure S3). The specificity of both the anti-HuR and anti-KSRP antibodies were validated for pull-down prior to use in our experiments (Figure S4). Thus, the successful pulldown of *FSTL1* using anti-HuR is likely to represent a specific interaction between this transcript and the HuR protein. Confirming the interaction between HuR and *FSTL1*, we set out to address the possibility that the U-rich motif (URE) in the 3'UTR of *FSTL1* is essential for this interaction (**Figure 3B**). To confirm that the URE sequence is required for this interaction, we performed RNA gel retardation assays using radiolabelled probes corresponding to the stem-loop precursor for miR-198 (pre-miR-198) or a mutant with five cytidine (C) residues replacing the URE and recombinant HuR (**Figure 3B**). Pre-miR-7, a known HuR target, was used as a positive control. Formation of RNA-protein complexes with pre-miR-7 and wild-type pre-miR-198 probes, but not with mutant probes confirmed the specificity of HuR binding to the

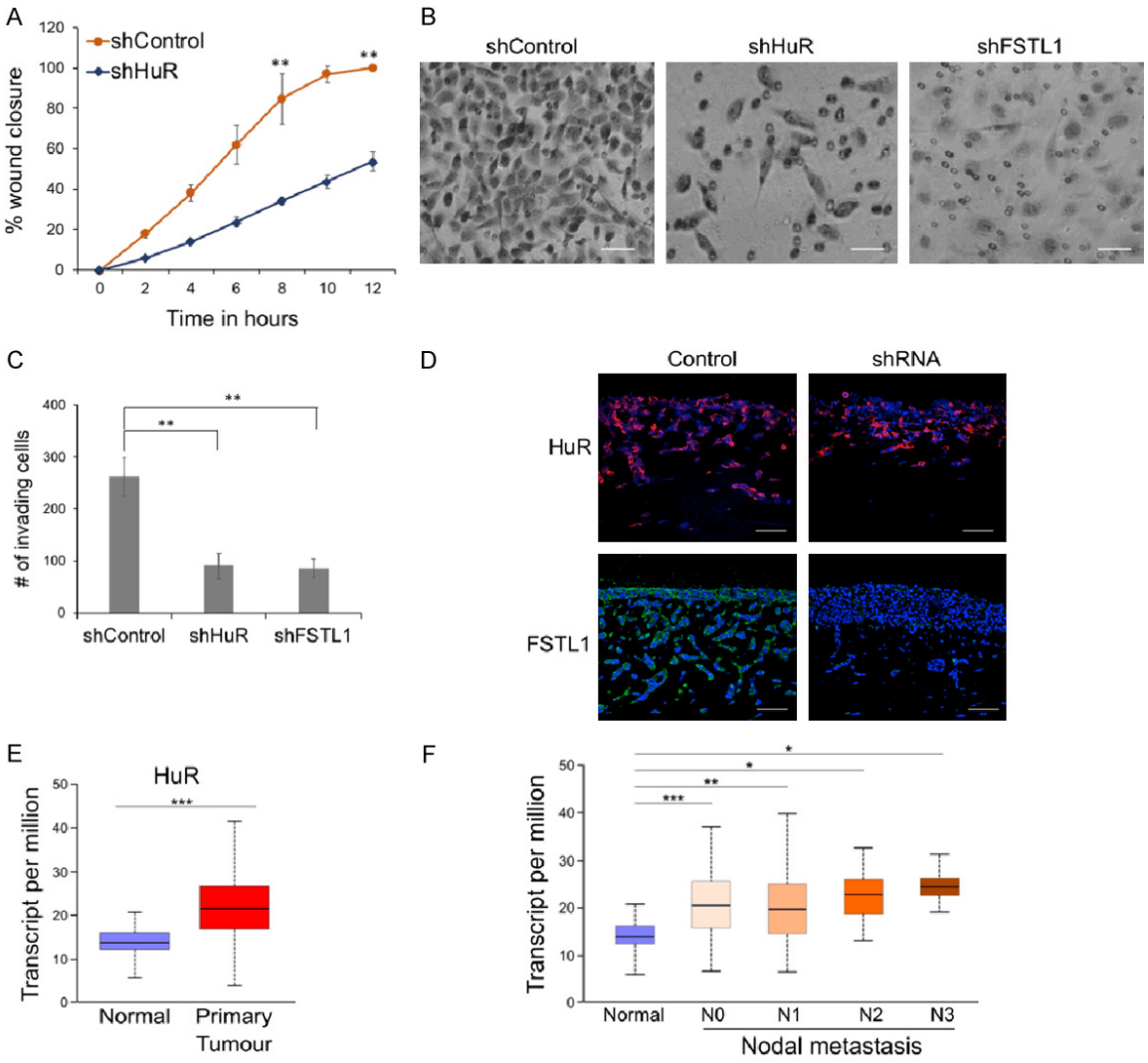

Figure 2. HuR is pro-invasive and knockdown of HuR phenocopies FSTL1 knockdown. A. Quantification of relative wound closure in SCC12 cells stably transduced with shHuR or control shRNA. Error bars represent SD. $^{**}P<0.01$. B. Boyden chamber invasion assay shows a significant decrease in the number of SCC12 cells invading the chamber matrix in shHuR- and shFSTL1-treated cells compared with control cells. Representative images of migrated cells detected with Giemsa staining. Scale bar = 10 μm. C. Bar graph showing the number of invading cells in Boyden chamber assay from six independent fields and three biological replicates. Error bars represent SD, $^{**}P<0.01$ (*t*-test). D. SCC invasion in an organotypic skin model in the presence of shHuR, shFSTL1 or control shRNA. (n=3). Scale bar =100 μm. E. Box-and-whisker plots showing HuR expression levels [transcripts per million, (TPM)] in healthy tissue (n=44) and SCC primary tumours (n=520) from TCGA database. F. Box-and-whisker plots showing HuR expression levels in healthy tissue (n=44) and SCC tumours classified by nodal metastasis status (N0: n=176, N1: n=67, N2: n=12, N3: n=8). $^{*}P<10^{-3}$, $^{**}P<10^{-5}$, $^{***}P<10^{-10}$ (*t*-test).

URE (**Figure 3C**). This inability of HuR to bind to the pre-miR-198 stem-loop in the absence of the U-rich motif confirms that the URE is essential for HuR-*FSTL1* interaction.

Given the close proximity between the URE (required for HuR binding) and the KSRP binding site (GUG) on pre-miR-198, we suspected that it might not be possible for both proteins to bind simultaneously. If this were the case, then KSRP and HuR could plausibly compete with each other to determine the fate of the *FSTL1* transcript. Competitive binding of proteins with alternative effects on RNA transcript stability has been documented in the regulation of unstable transcripts [25-27], with published effects on tumour progression. As HuR is overexpressed in squamous cell carcinoma,

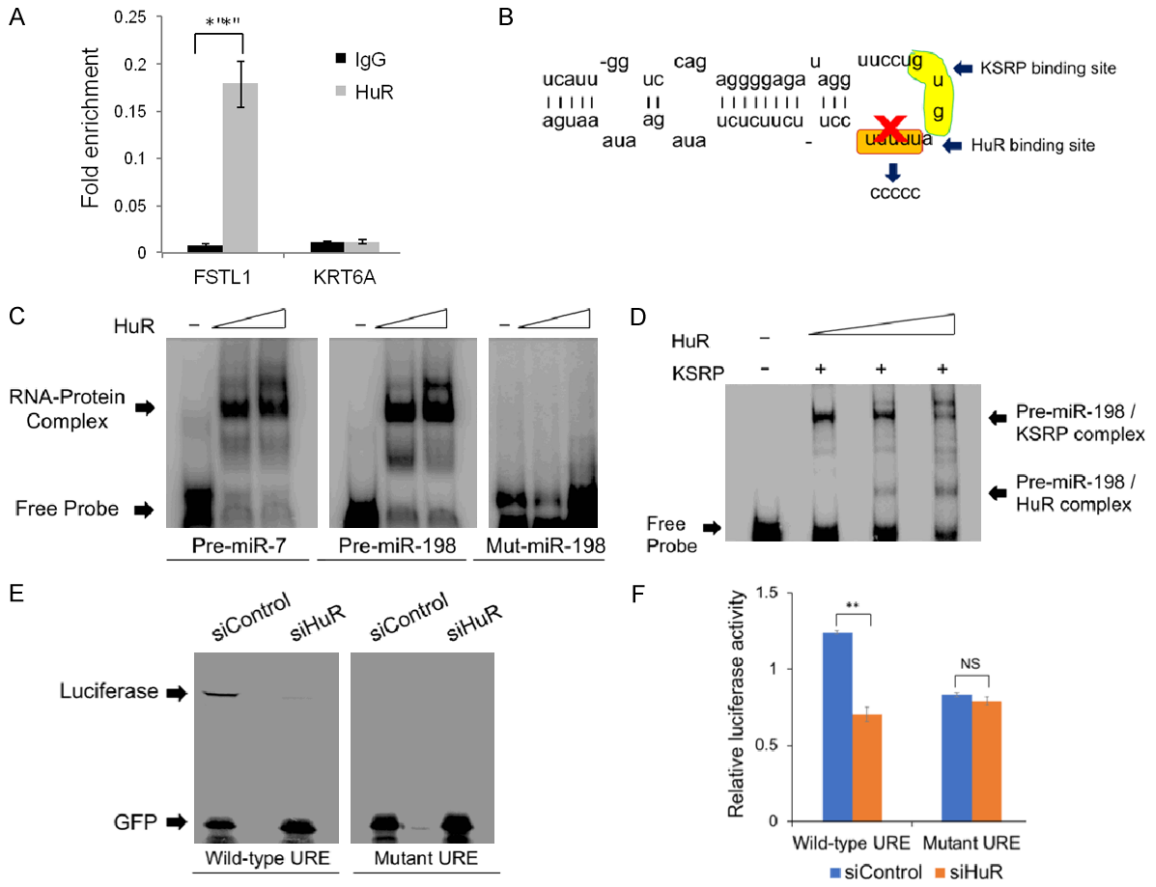

Figure 3. The interplay between two RNA-binding proteins controls the fate of *FSTL1* transcript. A. Fold enrichment of *FSTL1* and *KRT6A* in RNA immunoprecipitation assay on SCC12 cell lysate with anti-HuR antibody or IgG control. $^{**}P<0.01$ (*t*-test). B. Schematic illustration of the mutation of the URE element in pre-miR-198. C. RNA gel retardation assay with recombinant HuR and wild-type (WT) or mutant pre-miR-198 probes. Pre-miR-7 is a positive control. D. RNA gel retardation assay with recombinant HuR and KSRP using radio-labeled pre-miR-198 probes. KSRP was pre-incubated with pre-miR-198, then incubated with HuR (0.5, 2.0, and 5.0 μM). E. Autoradiography of *in vitro* translated products from chimeric luciferase assay with either WT or mutant *FSTL1* 3'-UTRs in the presence of lysate from SCC cells transfected with siHuR or siControl. *GFP* mRNA was co-translated in equal amounts as an endogenous control (n=3). F. Luciferase reporter assay with chimeric luciferase-*FSTL1* 3'-UTR constructs containing either a WT or mutant URE, co-transfected with siHuR or control siRNA. Bar graph represents relative luciferase activity at 24 h post-transfection, with firefly luciferase signal normalized to *Renilla* luciferase (endogenous control). n=3, $^{**}P<0.01$ (*t*-test).

we were interested in studying the effects of increased HuR concentration on KSRP binding. Wild-type pre-miR-198 was incubated with 0.5 μM recombinant KSRP, followed by the addition of HuR at different concentrations (0.5 μM, 2 μM, and 5 μM). RNA gel retardation revealed that increasing the concentration of HuR increases pre-miR-198-HuR complex formation as expected, and simultaneously reduces the formation of pre-miR-198-KSRP complexes (**Figure 3D**). This observation strongly indicates a competitive binding and HuR's ability to outcompete KSRP in SCC, where KSRP expression is significantly downregulated.

Having established that HuR binds to *FSTL1*, we determined the functional consequences of this interaction in stabilising *FSTL1* transcript. A luciferase open reading frame (ORF) was cloned upstream of a wild-type or mutant *FSTL1* 3'UTR. *In vitro* translation of this capped, chimeric transcript was performed in a rabbit reticulocyte system in the presence of lysate from SCC12 cells transfected with siRNA against HuR or control siRNA. Both HuR and wild-type URE are essential for luciferase expression-luciferase translation failed with the mutant UTR and was significantly reduced in response to HuR knockdown. No significant

expression differences were seen in co-translated *GFP* mRNA, which was used as a loading control and a control for target specificity (**Figure 3E**). From these observations, we infer that both HuR and the URE sequence are essential for FSTL1 translation.

Further evidence in support of this model comes from a luciferase assay on 293T cells co-transfected with either the wild-type or mutant constructs, and either siHuR or siControl. Firefly luciferase readings for each sample were normalised to those of *Renilla* luciferase (an endogenous control present in the same construct). We observed that, with the wild-type URE, downregulation of normalized luciferase activity was significantly greater in response to siHUR relative to siControl. Similarly, decreased luciferase activity was apparent with the mutant URE compared to the wild-type URE. HuR knockdown had no effect relative to the control in the presence of the mutant URE (**Figure 3F**), suggesting that HuR-mediated FSTL1 stabilization requires an intact URE.

HuR enhances stability of FSTL1 transcript and enables sustained FSTL1 protein expression in SCC

In SCC12 cells, upon transfection with siHuR, a significant reduction in both *HuR* and *FSTL1* transcript abundance relative to siControl was observed (**Figure 4A**). To provide direct evidence that the HuR-URE interaction stabilizes *FSTL1*, we assessed *FSTL1* degradation in SCC12 cells treated with Actinomycin D (ActD), a global transcription inhibitor. In the absence of de novo transcription a significant decrease in *FSTL1* transcript abundance was apparent in cells transfected with siHuR relative to the control confirming the role of HuR in maintaining FSTL1 transcript stability (**Figure 4B**). HuR's stabilizing effect on *FSTL1* mRNA is reflected in FSTL1 protein abundance. HuR knockdown substantially reduces FSTL1 protein expression (**Figure 4C**). In contrast, upon knockdown of KSRP we observed an increase in FSTL1 protein abundance (**Figure 4C**), all confirming the role of HuR in the stabilization of FSTL1.

These observations are congruent with the hypothesis that HuR and KSRP modulate the molecular switch through *FSTL1* stabilization and destabilization, respectively. In healthy epithelia, KSRP destabilizes *FSTL1* and prevents its translation. In SCC, HuR-mediated *FSTL1* stabilization enables sustained FSTL1 protein production. These effects on *FSTL1* transcript stability also directly affect the alternative switch product-the tumour suppressor miRNA miR-198. Knocking down HuR significantly increases miR-198 expression (**Figure 4D**). Thus, by piecing these observations together, we propose a model whereby abnormal HuR expression in tumours, coupled with EGF-mediated downregulation of KSRP, enables HuR to outcompete KSRP for binding to the *FSTL1* transcript. This stabilizes *FSTL1*, favouring FSTL1 translation and downregulating miR-198. The loss of miR-198 enables abnormal expression of its pro-migratory targets including DIAPH1, LAMC2 and PLAU (**Figure 4E**). These pro-invasive proteins act in synergy with FSTL1 to enhance invasion and metastasis in SCC (**Figure 4F**).

Discussion

The RNA-binding protein HuR (Human antigen R) is aberrantly expressed in a variety of malignancies, where it drives oncogenic progression and metastasis. HuR confers a wide array of functions in cancer cells, including enhanced cell proliferation [28, 29], hypoxia resistance [30, 31] and improved migratory capacity [32-34]. As metastasis is the leading cause of death in the majority of patients with epithelial cancer, we are particularly interested in the pro-metastatic effects of HuR. The targets of HuR, which are implicated in metastasis include matrix metalloproteinases [32, 34], regulators of epithelial-to-mesenchymal transition such as Snail [33], and genes with pleiotropic roles in carcinogenesis. Cyclooxygenase-2 (COX-2) is an example of a well-characterised pro-tumourigenic factor upregulated by HuR. Oncogenic roles of the HuR/COX-2 axis have been described in cancers of the larynx [35], lung [36], uterine cervix [37], thyroid [38], colon [39], as well as in mesothelioma [40]. In this study, we add to the growing body of data on HuR in metastasis by demonstrating how HuR acts as an upstream regulator of FSTL1; controls the fate of the FSTL1 transcript, enabling sustained expression of the pro-migratory and pro-metastatic glycoprotein, FSTL1.

FSTL1 is multifunctional, with a variety of roles in carcinogenesis. FSTL1 promotes immune

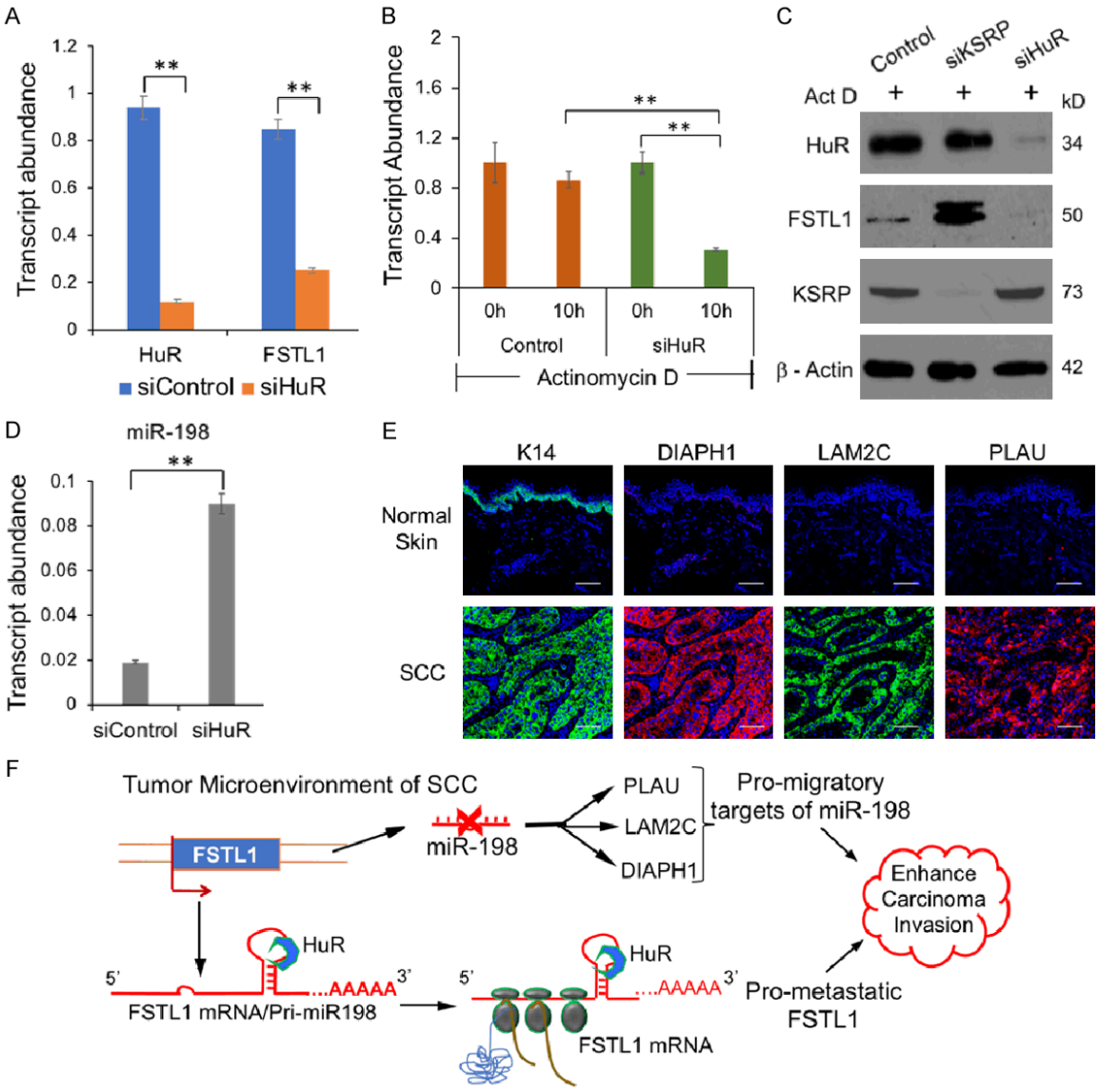

Figure 4. HuR enhances stability of FSTL1 transcript and enables sustained FSTL1 protein expression in SCC. A. Relative transcript abundance of *HuR* and *FSTL1* in SCC cells transfected with siHuR or siControl. B. *FSTL1* relative transcript abundance in SCC cells transfected with siHuR or siControl followed by Actinomycin D treatment. n=3, $^{**}P<0.01$ (t-test). C. Western blot showing KSRP, HuR, FSTL1, and β-actin (loading control) in SCC12 cells transfected with siKSRP, siHuR, or control siRNA (n=3). D. Relative transcript abundance of miR-198 in SCC12 cells transfected with siHuR or siControl. n=3, $^{**}P<0.01$ (t-test). E. Immunofluorescence staining for KRT14 (control), PLAU, LAMC2, and DIAPH1 on normal skin (n=5) and SCC (n=86) sections. Scale =100 μm. F. Model depicting HuR-mediated modulation of the wound healing switch in SCC. Unless otherwise stated, all error bars denote ± SEM.

evasion by cancer cells [41]. In squamous cell carcinoma (SCC), FSTL1 drives metastasis by upregulating matrix metalloproteinase 9 (MMP9) via the ERK (extracellular signal-regulated kinase) signalling pathway [2]. Notably, HuR has also been reported to enhance metastasis by acting through MMP9 [32, 42]. Although these studies focused on HuR's stabilization of MMP9 itself, it is possible that HuR-mediated *FSTL1* stabilization acting upstream of MMP9 may have a direct impact on metastasis. FSTL1's pro-metastatic effects in SCC occur in synergy with the loss of the anti-migratory microRNA miR-198 [2]. The mutually exclusive production of either miR-198 or FSTL1 from the same parental transcript allows for the existence of a bistable on/off molecular switch for keratinocyte migration [1]. We have

previously shown that KSRP-mediated destabilization of this transcript is essential for miR-198 production at steady state in the healthy epithelium, and that the loss of KSRP in the context of both SCC [2] and normal wound healing [1] cause keratinocytes to adopt a pro-migratory phenotype. Our study highlights the role of HuR in this process and addresses the outstanding question on whether KSRP down-regulation alone is sufficient for the sustained FSTL1 expression in SCC. KSRP functions as a miRNA processing factor to ensure miR-198 production in healthy epithelia; its loss is permissive, but not sufficient, for persistent enhanced expression of FSTL1 in SCC. The antagonistic roles played by HuR and KSRP in determining transcript fate is not unique to *FSTL1* - both proteins also perform similar roles in determining *IL-8* transcript stability in breast cancer cells [27]. In this case, *IL-8* stability increases following stimulation with IL-1β or TNF-α due to greater association of HuR to IL-8 transcript relative to KSRP.

Our observation that HuR contributes to regulating keratinocyte migration via the miR-198/FSTL1 switch raises the possibility that HuR may also regulate another linked biological process - wound healing. The cell behaviours that enable epithelial repair following injury are remarkably similar to those that enable tumour cell dissemination, as are the molecular pathways that regulate such behaviours [2]. The miR-198/FSTL1 switch and its reliance on KSRP were originally identified in the context of epithelial wound repair [1]. Despite these similarities, wound healing and metastasis differ fundamentally in their outcomes - the former is self-limiting and essential to the maintenance of homeostasis, whilst the latter is the pathological result of failure to regulate cell migration. Regulatory differences exist between both processes, and the involvement of HuR may be one such discrepancy.

From a clinical perspective, the possibility of using HuR as a target for anticancer therapy has been broached by several authors [16, 43] due to its central role in enabling multiple cancer phenotypes. Our findings concur with these perspectives. However, as HuR is a multifunctional RNA-binding protein with pleiotropic roles in multiple pathways and hence, targeting HuR may have unforeseen detrimental effects. In the context of the model we have presented, targeting FSTL1 as a downstream effector of HuR in SCC would reduce the risk of metastasis whilst providing a more refined approach that minimises risks associated with HuR inhibition. Thus, we propose that a suitable FSTL1 inhibitor, coupled with a compound that simultaneously restores the expression of tumour suppressor-miR-198, may be of significant clinical benefit in limiting metastatic dissemination. As the majority of cancer-related deaths arise from complications due to metastasis, we envisage that this therapeutic strategy would substantially reduce morbidity and mortality attributable to squamous cell carcinoma.

Acknowledgements

This work was supported by National Medical Research Council (NMRC)-Open Fund Individual Research Grant (OFIRG/0047/2017) to PS and Biomedical Research Council of Singapore, A*STAR. We would like to thank Dr. E Birgitte Lane and Dr. John Common for graciously providing us cSCC cell lines.

Disclosure of conflict of interest

None.

Abbreviations

ARE, Adenylate-rich element; EGF, Epidermal growth factor; FSTL1, Follistatin-like 1; KSRP, KH-type splicing regulatory protein; KRT6A, Keratin 6A; HuR, Human Antigen R; ORF, Open reading frame; RIP, RNA immunoprecipitation; RRM, RNA recognition motif; SCC, Squamous cell carcinoma; shRNA, Short hairpin RNA; TCGA, The Cancer Genome Atlas; URE, Uridylate-rich element.

Address correspondence to: Dr. Prabha Sampath, Skin Research Institute of Singapore, Agency for Science Technology & Research (A*STAR), 8A Biomedical Grove, #05-41 Immunos, Singapore 138648, Singapore. Tel: +65-6407-0171; E-mail: prabha.sampath@sris.a-star.edu.sg

References

[1] Sundaram GM, Common JE, Gopal FE, Srikanta S, Lakshman K, Lunny DP, Lim TC, Tanavde V, Lane EB and Sampath P. 'See-saw' expression of microRNA-198 and FSTL1 from a single

transcript in wound healing. Nature 2013; 495: 103-106.
[2] Sundaram GM, Ismail HM, Bashir M, Muhuri M, Vaz C, Nama S, Ow GS, Vladimirovna IA, Ramalingam R, Burke B, Tanavde V, Kuznetsov V, Lane EB and Sampath P. EGF hijacks miR-198/FSTL1 wound-healing switch and steers a two-pronged pathway toward metastasis. J Exp Med 2017; 214: 2889-2900.
[3] Bevivino G, Sedda S, Franze E, Stolfi C, Di Grazia A, Dinallo V, Caprioli F, Facciotti F, Colantoni A, Ortenzi A, Rossi P and Monteleone G. Follistatin-like protein 1 sustains colon cancer cell growth and survival. Oncotarget 2018; 9: 31278-31290.
[4] Lau MC, Ng KY, Wong TL, Tong M, Lee TK, Ming XY, Law S, Lee NP, Cheung AL, Qin YR, Chan KW, Ning W, Guan XY and Ma S. FSTL1 promotes metastasis and chemoresistance in esophageal squamous cell carcinoma through NFkappaB-BMP signaling cross-talk. Cancer Res 2017; 77: 5886-5899.
[5] Kudo-Saito C. FSTL1 promotes bone metastasis by causing immune dysfunction. Oncoimmunology 2013; 2: e26528.
[6] Minafra L, Bravata V, Forte GI, Cammarata FP, Gilardi MC and Messa C. Gene expression profiling of epithelial-mesenchymal transition in primary breast cancer cell culture. Anticancer Res 2014; 34: 2173-2183.
[7] Trojan L, Schaaf A, Steidler A, Haak M, Thalmann G, Knoll T, Gretz N, Alken P and Michel MS. Identification of metastasis-associated genes in prostate cancer by genetic profiling of human prostate cancer cell lines. Anticancer Res 2005; 25: 183-191.
[8] Kudo-Saito C, Ishida A, Shouya Y, Teramoto K, Igarashi T, Kon R, Saito K, Awada C, Ogiwara Y and Toyoura M. Blocking the FSTL1-DIP2A axis improves anti-tumor immunity. Cell Rep 2018; 24: 1790-1801.
[9] Ripin N, Boudet J, Duszczyk MM, Hinniger A, Faller M, Krepl M, Gadi A, Schneider RJ, Sponer J, Meisner-Kober NC and Allain FH. Molecular basis for AU-rich element recognition and dimerization by the HuR C-terminal RRM. Proc Natl Acad Sci U S A 2019; 116: 2935-2944.
[10] Chen CY, Xu N and Shyu AB. Highly selective actions of HuR in antagonizing AU-rich element-mediated mRNA destabilization. Mol Cell Biol 2002; 22: 7268-7278.
[11] Good PJ. A conserved family of elav-like genes in vertebrates. Proc Natl Acad Sci U S A 1995; 92: 4557-4561.
[12] Scheiba RM, de Opakua AI, Diaz-Quintana A, Cruz-Gallardo I, Martinez-Cruz LA, Martinez-Chantar ML, Blanco FJ and Diaz-Moreno I. The C-terminal RNA binding motif of HuR is a multifunctional domain leading to HuR oligomerization and binding to U-rich RNA targets. RNA Biol 2014; 11: 1250-1261.
[13] Fus LP, Pihowicz P, Koperski L, Marczewska JM and Gornicka B. High cytoplasmic HuR expression is associated with advanced pT stage, high grade and increased microvessel density in urothelial bladder carcinoma. Ann Diagn Pathol 2018; 33: 40-44.
[14] Liu Y, Chen X, Cheng R, Yang F, Yu M, Wang C, Cui S, Hong Y, Liang H, Liu M, Zhao C, Ding M, Sun W, Liu Z, Sun F, Zhang C, Zhou Z, Jiang X and Chen X. The Jun/miR-22/HuR regulatory axis contributes to tumourigenesis in colorectal cancer. Mol Cancer 2018; 17: 11.
[15] Palomo-Irigoyen M, Perez-Andres E, Iruarrizaga-Lejarreta M, Barreira-Manrique A, Tamayo-Caro M, Vila-Vecilla L, Moreno-Cugnon L, Beitia N, Medrano D, Fernandez-Ramos D, Lozano JJ, Okawa S, Lavin JL, Martin-Martin N, Sutherland JD, de Juan VG, Gonzalez-Lopez M, Macias-Camara N, Mosen-Ansorena D, Laraba L, Hanemann CO, Ercolano E, Parkinson DB, Schultz CW, Arauzo-Bravo MJ, Ascension AM, Gerovska D, Iribar H, Izeta A, Pytel P, Krastel P, Provenzani A, Seneci P, Carrasco RD, Del Sol A, Martinez-Chantar ML, Barrio R, Serra E, Lazaro C, Flanagan AM, Gorospe M, Ratner N, Aransay AM, Carracedo A, Varela-Rey M and Woodhoo A. HuR/ELAVL1 drives malignant peripheral nerve sheath tumor growth and metastasis. J Clin Invest 2020; 130: 3848-3864.
[16] Wang J, Guo Y, Chu H, Guan Y, Bi J and Wang B. Multiple functions of the RNA-binding protein HuR in cancer progression, treatment responses and prognosis. Int J Mol Sci 2013; 14: 10015-10041.
[17] Zhang Y, Yang L, Ling C and Heng W. HuR facilitates cancer stemness of lung cancer cells via regulating miR-873/CDK3 and miR-125a-3p/CDK3 axis. Biotechnol Lett 2018; 40: 623-631.
[18] Xu X, Song C, Chen Z, Yu C, Wang Y, Tang Y and Luo J. Downregulation of HuR inhibits the progression of esophageal cancer through interleukin-18. Cancer Res Treat 2018; 50: 71-87.
[19] Kim KY, Li S, Cha JD, Zhang X and Cha IH. Significance of molecular markers in survival prediction of oral squamous cell carcinoma. Head Neck 2012; 34: 929-936.
[20] Zhang C, Xue G, Bi J, Geng M, Chu H, Guan Y, Wang J and Wang B. Cytoplasmic expression of the ELAV-like protein HuR as a potential prognostic marker in esophageal squamous cell carcinoma. Tumour Biol 2014; 35: 73-80.
[21] Abdelmohsen K and Gorospe M. Posttranscriptional regulation of cancer traits by HuR. Wiley Interdiscip Rev RNA 2010; 1: 214-229.
[22] Hu YP, Jin YP, Wu XS, Yang Y, Li YS, Li HF, Xiang SS, Song XL, Jiang L, Zhang YJ, Huang W, Chen

SL, Liu FT, Chen C, Zhu Q, Chen HZ, Shao R and Liu YB. LncRNA-HGBC stabilized by HuR promotes gallbladder cancer progression by regulating miR-502-3p/SET/AKT axis. Mol Cancer 2019; 18: 167.

[23] Zhang Z, Huang A, Zhang A and Zhou C. HuR promotes breast cancer cell proliferation and survival via binding to CDK3 mRNA. Biomed Pharmacother 2017; 91: 788-795.

[24] Nystrom ML, Thomas GJ, Stone M, Mackenzie IC, Hart IR and Marshall JF. Development of a quantitative method to analyse tumour cell invasion in organotypic culture. J Pathol 2005; 205: 468-475.

[25] Lal A, Mazan-Mamczarz K, Kawai T, Yang X, Martindale JL and Gorospe M. Concurrent versus individual binding of HuR and AUF1 to common labile target mRNAs. EMBO J 2004; 23: 3092-3102.

[26] Linker K, Pautz A, Fechir M, Hubrich T, Greeve J and Kleinert H. Involvement of KSRP in the post-transcriptional regulation of human iNOS expression-complex interplay of KSRP with TTP and HuR. Nucleic Acids Res 2005; 33: 4813-4827.

[27] Suswam EA, Nabors LB, Huang Y, Yang X and King PH. IL-1beta induces stabilization of IL-8 mRNA in malignant breast cancer cells via the 3' untranslated region: involvement of divergent RNA-binding factors HuR, KSRP and TIAR. Int J Cancer 2005; 113: 911-919.

[28] Guo X and Hartley RS. HuR contributes to cyclin E1 deregulation in MCF-7 breast cancer cells. Cancer Res 2006; 66: 7948-7956.

[29] Kim HH, Yang X, Kuwano Y and Gorospe M. Modification at HuR(S242) alters HuR localization and proliferative influence. Cell Cycle 2008; 7: 3371-3377.

[30] Galban S, Kuwano Y, Pullmann R Jr, Martindale JL, Kim HH, Lal A, Abdelmohsen K, Yang X, Dang Y, Liu JO, Lewis SM, Holcik M and Gorospe M. RNA-binding proteins HuR and PTB promote the translation of hypoxia-inducible factor 1alpha. Mol Cell Biol 2008; 28: 93-107.

[31] Levy NS, Chung S, Furneaux H and Levy AP. Hypoxic stabilization of vascular endothelial growth factor mRNA by the RNA-binding protein HuR. J Biol Chem 1998; 273: 6417-6423.

[32] Akool el S, Kleinert H, Hamada FM, Abdelwahab MH, Forstermann U, Pfeilschifter J and Eberhardt W. Nitric oxide increases the decay of matrix metalloproteinase 9 mRNA by inhibiting the expression of mRNA-stabilizing factor HuR. Mol Cell Biol 2003; 23: 4901-4916.

[33] Dong R, Lu JG, Wang Q, He XL, Chu YK and Ma QJ. Stabilization of Snail by HuR in the process of hydrogen peroxide induced cell migration. Biochem Biophys Res Commun 2007; 356: 318-321.

[34] Huwiler A, Akool el S, Aschrafi A, Hamada FM, Pfeilschifter J and Eberhardt W. ATP potentiates interleukin-1 beta-induced MMP-9 expression in mesangial cells via recruitment of the ELAV protein HuR. J Biol Chem 2003; 278: 51758-51769.

[35] Cho NP, Han HS, Soh Y, Lee KY and Son HJ. Cytoplasmic HuR over-expression is associated with increased cyclooxygenase-2 expression in laryngeal squamous cell carcinomas. Pathology 2007; 39: 545-550.

[36] Kim GY, Lim SJ and Kim YW. Expression of HuR, COX-2, and survivin in lung cancers; cytoplasmic HuR stabilizes cyclooxygenase-2 in squamous cell carcinomas. Mod Pathol 2011; 24: 1336-1347.

[37] Lim SJ, Kim HJ, Kim JY, Park K and Lee CM. Expression of HuR is associated with increased cyclooxygenase-2 expression in uterine cervical carcinoma. Int J Gynecol Pathol 2007; 26: 229-234.

[38] Giaginis C, Alexandrou P, Delladetsima I, Karavokyros I, Danas E, Giagini A, Patsouris E and Theocharis S. Clinical significance of Hu-Antigen Receptor (HuR) and Cyclooxygenase-2 (COX-2) expression in human malignant and benign thyroid lesions. Pathol Oncol Res 2016; 22: 189-196.

[39] Young LE, Sanduja S, Bemis-Standoli K, Pena EA, Price RL and Dixon DA. The mRNA binding proteins HuR and tristetraprolin regulate cyclooxygenase 2 expression during colon carcinogenesis. Gastroenterology 2009; 136: 1669-1679.

[40] Stoppoloni D, Cardillo I, Verdina A, Vincenzi B, Menegozzo S, Santini M, Sacchi A, Baldi A and Galati R. Expression of the embryonic lethal abnormal vision-like protein HuR in human mesothelioma: association with cyclooxygenase-2 and prognosis. Cancer 2008; 113: 2761-2769.

[41] Kudo-Saito C, Fuwa T, Murakami K and Kawakami Y. Targeting FSTL1 prevents tumor bone metastasis and consequent immune dysfunction. Cancer Res 2013; 73: 6185-6193.

[42] Hua X, Chen L, Wang J, Li J and Wingender E. Identifying cell-specific microRNA transcriptional start sites. Bioinformatics 2016; 32: 2403-10.

[43] Wu M, Tong CWS, Yan W, To KKW and Cho WCS. The RNA binding protein HuR: a promising drug target for anticancer therapy. Curr Cancer Drug Targets 2019; 19: 382-399.

Table S1. List of oligonucleotides used in this study

Primer	Sequence	Target
Luciferase T7 forward	TAATACGACTCACTATAGGG AAA GCC ACC ATG GAA GAT GCC	Binds 9 bp upstream of Luciferase AUG in pMIRGLO. Includes the Kozak sequence
FSTL1 3'UTR reverse	CCG AAA AGG AAG AAT CAG GAG	Binds to position 2617 in FSTL1 3'UTR
CopGFP start T7F	TAATACGACTCACTATAGGG cta gac gcc acc atg gag agc	
CopGFP stop R	GTCGACTTAGCGAGATCCGGTG	
T7 pre-miR-7 F	TAATACGACTCACTATAGGG ttggatgttg gcctagttct	
Pre-miR-7 R	CTGTAGAGGCATGGCCTGTG	

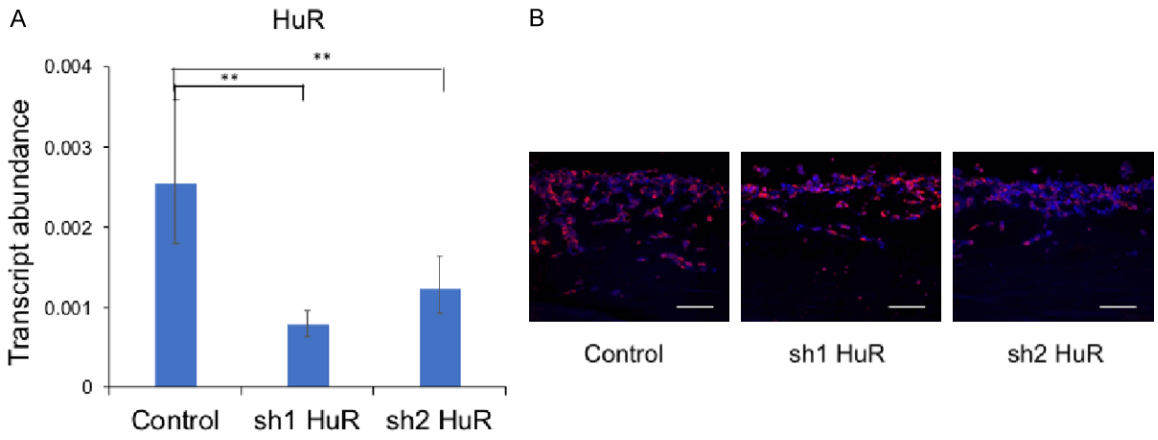

Figure S1. Validation of shHuR. A. Bar graph shows transcript abundance of HuR in SCC12 cells transduced with sh1 HuR and sh2 HuR. B. SCC invasion in an organotypic skin model in the presence of sh1 HuR, sh2 HuR or control shRNA (n=3), Scale bar =100 μm.

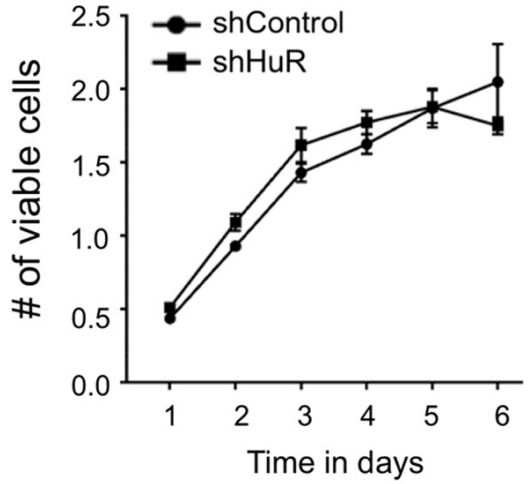

Figure S2. HuR knock down does not affect the proliferation of SCC cells. SCC cells transfected with control shRNA or shHuR were seeded on 96 well plates at low density and cell proliferation was measured post seeding by Cell Titer Glo assay. No significant difference in proliferation was observed between control and shHuR cells.

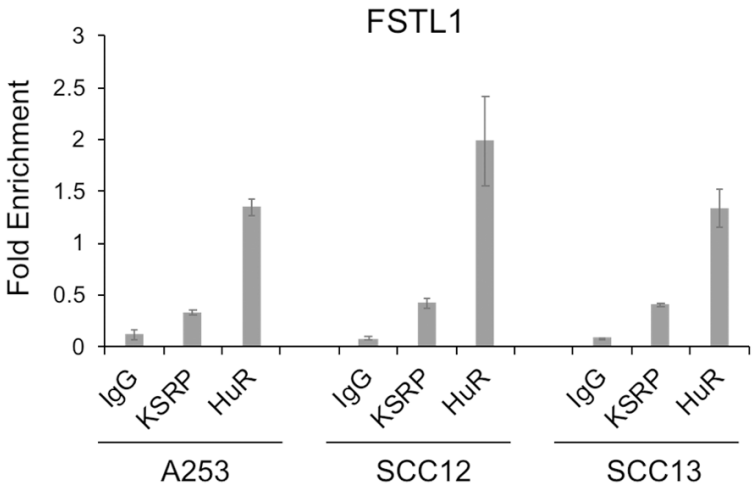

Figure S3. Bar graph showing fold enrichment of the *FSTL1* transcript resulting from RIP with control IgG, anti-KSRP, and anti-HuR antibodies. The experiment was performed in the A253, SCC12, and SCC13 cell lines.

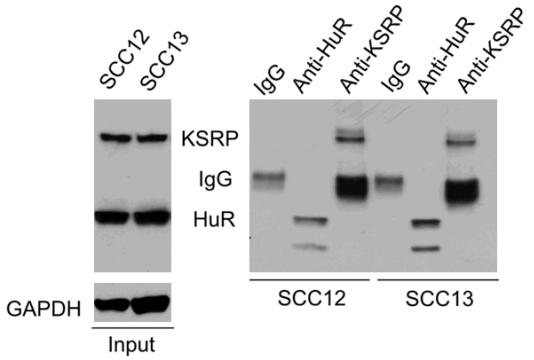

Figure S4. Validation of immunoprecipitation using anti-HuR and anti-KSRP antibodies. Total cell extracts from SCC cell lines were subjected to co-immunoprecipitation using anti-HuR, anti-KSRP and control IgG antibodies. After the immunoprecipitation of antibody bound complexes, a fraction of samples were subjected to western blot using anti-HuR (rabbit) and anti-KSRP (rabbit) antibodies. Left panel shows the specific immunoprecipitation of HuR and KSRP with its respective antibodies while control IgG did not pull down these proteins. Total cell extracts were evaluated for HuR, KSRP and GAPDH.